HIPPOCAMPUS 11:204–215 (2001)

Phase Precession and Phase-Locking of Hippocampal Pyramidal Cells

Amitabha Bose[1,*] and Michael Recce[1,2]

[1]*Department of Mathematical Sciences, Center for Applied Mathematics and Statistics, New Jersey Institute of Technology, Newark, New Jersey*
[2]*Department of Computer Science, Center for Computational Biology and Bioengineering, New Jersey Institute of Technology, Newark, New Jersey*

ABSTRACT: We propose that the activity patterns of CA3 hippocampal pyramidal cells in freely running rats can be described as a temporal phenomenon, where the timing of bursts is modulated by the animal's running speed. With this hypothesis, we explain why pyramidal cells fire in specific spatial locations, and how place cells phase-precess with respect to the EEG theta rhythm for rats running on linear tracks. We are also able to explain why wheel cells phase-lock with respect to the theta rhythm for rats running in a wheel. Using biophysically minimal models of neurons, we show how the same network of neurons displays these activity patterns. The different rhythms are the result of inhibition being used in different ways by the system. The inhibition is produced by anatomically and physiologically diverse types of interneurons, whose role in controlling the firing patterns of hippocampal cells we analyze. Each firing pattern is characterized by a different set of functional relationships between network elements. Our analysis suggests a way to understand these functional relationships and transitions between them. ***Hippocampus 2001;11:204–215.*** **© 2001 Wiley-Liss, Inc.**

KEY WORDS: place cell; wheel cell; temporal code; biophysical model

INTRODUCTION

Pyramidal cells in region CA3 of the hippocampus of rats have long been the focus of research, in part, because of the behaviorally correlated firing patterns that they exhibit. For example, as a rat explores an environment, pyramidal cells in its hippocampus fire transiently in spatially specific locations called "place fields" (O'Keefe and Dostrovsky, 1971). These pyramidal cells are called "place cells," and their firing rate is highest when the animal is in the center of the place field. As the animal's distance from the center of the place field decreases, the firing rate decreases (but see also Mehta et al., 2000). Recently, Czurkó et al. (1999) demonstrated that pyramidal cells fire tonically when the rat is running "space-clamped" inside of a running wheel. These pyramidal cells behave like place cells in the sense that translation or rotation of the wheel relative to the background cues causes the pyramidal cells to stop firing. Czurkó et al. (1999) called these cells "wheel cells." In either case, the firing of pyramidal cells can be interpreted as a rate code for spatial location of the animal (Brown et al., 1998; Zhang et al., 1998).

Place-cell firing also displays a phase-based code (O'Keefe and Recce, 1993; Skaggs et al., 1996). O'Keefe and Recce (1993) found that place cells, in rats running on a linear runway, exhibit up to 360° of phase precession relative to the background hippocampal theta rhythm. They also found that the phase of firing of place cells is better correlated with the spatial location of the rat, as opposed to the time the rat spends in the place field. Alternatively, Hirase et al. (1999) reported that wheel cells do not phase-precess relative to the theta rhythm. This latter result is consistent with a phase-precession code, since in the wheel, the animal's spatial location is fixed.

These data suggest that while the rat is running, a particular pyramidal cell can display at least three types of different behavior: transient phase-precessed firing when the animal is in the place field of that cell, tonic phase-locked firing when the animal is running in the wheel, and little or no firing when the animal is outside either of these two locations.

In this paper, we investigate neural mechanisms which may be responsible for how and why pyramidal cells exhibit these three firing patterns. Our primary focus is to study this question in the context of the phase-precession phenomenon. We use biophysical models of conductance-based neurons to understand the dynamics of cells. We show that there are a number of small network models which are all capable of producing the behavior described above. Each of these models is consistent with the known anatomy of region CA3, and each suggests neural mechanisms and accompanying functional relationships which underlie the different rhythms.

A primary advantage of this modeling approach is that it leads to a number of concrete and testable experiments which we describe in the Discussion. A second aspect of our work is that it shows how networks of neurons can

Grant sponsor: NSF; Grant number: 9973230; Grant sponsor: NJIT; Grant numbers: 421540, 421920.
*Correspondence to: Amitabha Bose, Department of Mathematical Sciences, New Jersey Institute of Technology, Newark, NJ 07102-1982.
E-mail: bose@m.njit.edu
Accepted for publication 25 August 2000

© *2001 WILEY-LISS, INC.*

output information about a larger spatial extent than was present in the input to the network. Specifically, we show how a network which is given information only about the spatial location of the beginning of the place field and the velocity of the animal can determine the end of the place field of that cell, together with the location of the animal within the place field at all moments in time. The synthesized output of these distinct inputs is the phase-precession code, which we show is intimately linked with the existence and size of hippocampal place fields.

MODEL AND METHODS

The basic anatomy of the hippocampus and related brain regions is relatively well-understood. The medial septum provides a significant projection to the CA3 region of the hippocampus (Swanson and Cowan, 1976; Alonso and Kohler, 1982), including an inhibitory input that terminates on interneurons (Freund and Buzsáki, 1996) and a long-lasting cholinergic excitation to pyramidal cells (Shute and Lewis, 1963). The dentate granule cells are known to make excitatory synapses in a narrow transverse band to 14–17 pyramidal cells (Claiborne et al., 1986). Pyramidal cells in region CA3 have largely homogeneous physiology and make sparse excitatory synapses on one another and also on interneurons. In contrast, there is a considerable amount of heterogeneity in the types of interneurons in CA3 in both their intrinsic and synaptic properties (Freund and Buzsáki, 1996). Interneurons target both pyramidal cells and other interneurons with inhibitory synapses.

We consider three different network architectures (I–III) to illustrate the basic ideas behind phase precession and phase locking. By presenting multiple networks, we hope to emphasize that the ideas linking control, precession, and locking are not tied to one specific network architecture, but are more robust. The minimal models of CA3 and associated regions that we shall consider are consistent with the known anatomy and consist of one pyramidal cell (P), one or two interneurons (I_1 and I_2), a dentate granule cell (D), and a pacemaker input (T). We only model a single cell of each type, since we assume that the cell corresponds to an assembly of cells of the same type. In the case of the pyramidal cell, this cell assembly corresponds to the set of place cells which fire in the same location in an environment. The basic intrinsic and synaptic properties are described below.

Intrinsic Properties

Each network element is described by sets of voltage-gated conductance equations. The membrane voltages are determined by an inward, instantaneously activating conductance that does not inactivate and an outward current with time-dependent activation. All cells contain a passive leak current as well as a constant, external applied current that maintains the intrinsic, qualitative behaviors of the cells (see Appendix).

The pyramidal cell

P is modeled either as a conditional oscillator (network I) or as an intrinsic oscillator (networks II and III). In network I, P possesses a high-threshold inward current, representing, for example, a high-threshold calcium current (Wong and Prince, 1978; Traub and Miles, 1991) or synaptic excitation coming from other coactive place cells. This current is activated only when P fires and is renewed with each action potential. We assume that the current persists for about one theta cycle, thus providing P with sufficient depolarization to oscillate without outside input. In networks II and III, we simply assume that P is an oscillator.

The interneurons

We assume that all interneurons are intrinsically excitable, and do not fire action potentials unless they receive input from the network.

The pacemaker

During movement through an environment, extracellular activity in the rat hippocampus is dominated by the theta rhythm. There is general agreement that the medial septum is the primary pacemaker for this activity. We model this input as a single pacemaker T. We do not require a specific form for this input other than that it is rhythmic and oscillates at the theta frequency. It could correspond to a direct inhibitory input from the medial septum, or it could be downstream from this input.

The dentate granule cell

We also model D as an oscillator at the theta frequency. The intrinsic dynamics of D are relatively unimportant for the functioning of the model, but its synaptic dynamics are crucial. The D cell, as described above, may correspond to a set of dentate granule cells. When these cells are coactive, they convey spatial information to pyramidal cells, which signals the start of the place field. We assume that this set of cells reliably activates the corresponding place-cell assembly.

Synaptic Properties and Architecture

Activation of the synaptic currents between cells depends on presynaptic voltage and is governed by a single equation with constant rise and decay rates as in Wang and Rinzel (1992) (see Appendix). In all of the networks, T targets the interneurons with fast-decaying inhibition; D targets P with fast-decaying excitation. Dentate granule cells have small place fields relative to the size of pyramidal cell place fields (Jung and McNaughton, 1993). Moreover, Skaggs et al. (1996) showed that dentate granule cells always begin to fire at a fixed particular phase of the theta rhythm. We interpret these two observations as meaning that the synaptic pathway from D to P provides excitatory input only at the beginning of a pyramidal cell place field. The data of Skaggs et al. (1996) suggest that dentate cells phase-precess for the few cycles during which they fire. We do not utilize this observation, but note that our

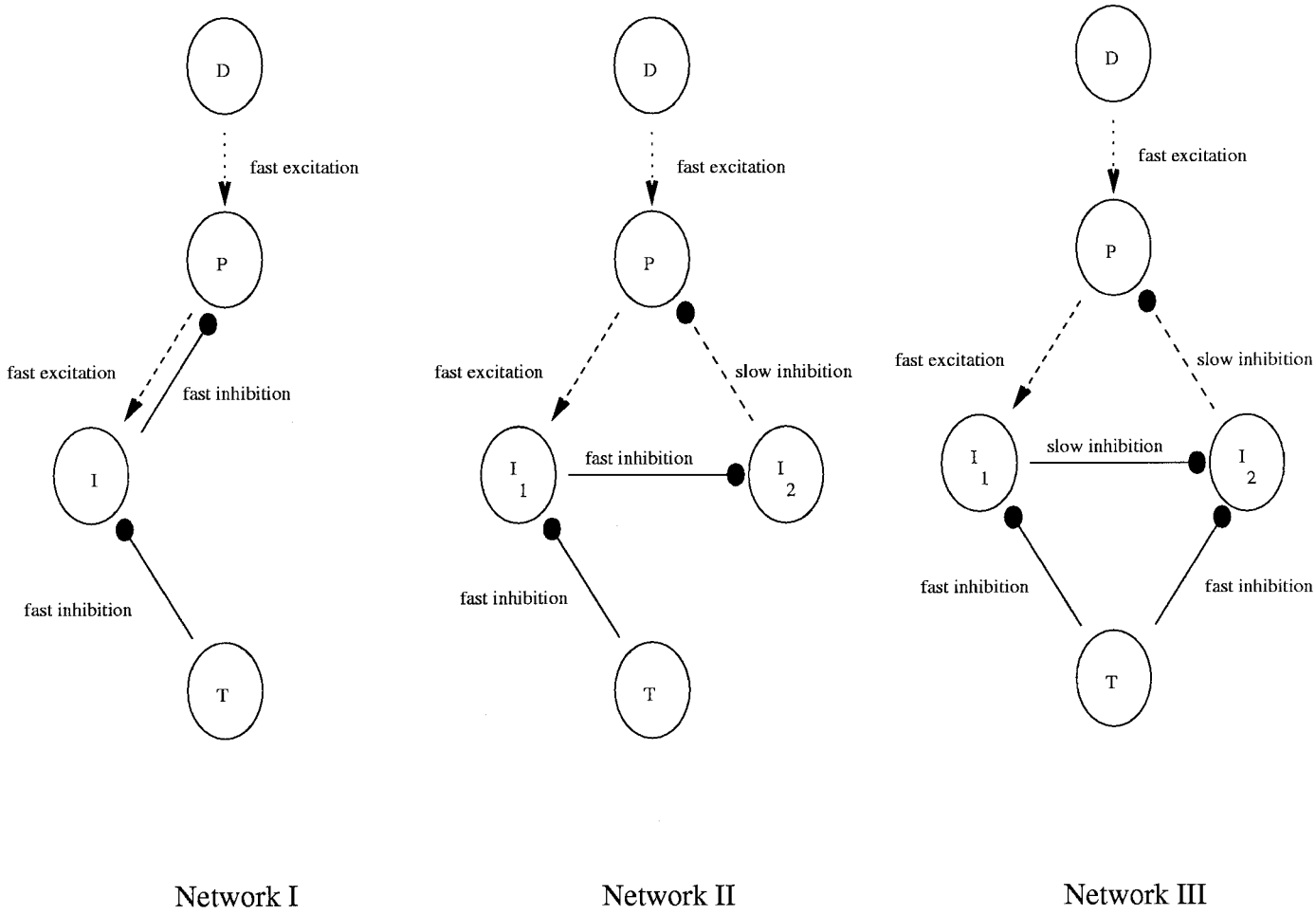


FIGURE 1. Architecture of networks I–III. Lines indicate synaptic connections. Solid circles are inhibitory, and arrows are excitatory. Synaptic connections are fast-acting, and some have a longer efficacy, as indicated. Some of the connections (dashed and dotted lines) have short intervals in which the synaptic input has physiological significance. The synapse from *D* to *P* is only active at the beginning of a place field. The maximal conductances of all synapses, except for that from *D* to *P*, is constant for all time.

results will not change qualitatively were we to add this to our models.

Each network (see Fig. 1) has a minimal number of synaptic connections necessary to obtain the desired network output. As we specify below, the addition of certain other synaptic connections do not change the results. As will become apparent, the neglected synaptic connections never become functionally relevant, because the synaptic current arrives at the postsynaptic cell at a time when it has little or no effect.

Network I

For this case, we require only one interneuron I. This interneuron receives fast decaying inhibition from T and provides fast-decaying inhibition to P. The interneuron receives fast-decaying excitation from P. The interneuron has the property that it can fire an action potential due to either the excitatory input from P or from the inhibitory input from T by postinhibitory rebound.

Network II

There are two interneurons, I_1 and I_2. I_1 receives fast-decaying inhibition from T and fast-decaying excitation from P, as above. I_1 provides fast-decaying inhibition to I_2, while I_2 sends slowly decaying inhibition to P. The model results do not change if there is a fast- or slow-decaying inhibition from I_1 to P, or if there is a fast- or slow-decaying inhibition from I_2 to I_1. An important aspect of this model is that I_2 will fire an action potential if and only if I_1 fires by postinhibitory rebound. If I_1 fires by postinhibitory rebound, then it will have a wider action potential, which means it will inhibit I_2 longer. This longer-lasting inhibition is sufficient to allow I_2 to fire a rebound spike.

Network III

Both interneurons I_1 and I_2 receive fast-decaying inhibition from T. I_2 sends slowly decaying inhibition to P, but now receives slowly decaying inhibition from I_1. I_1 is the recipient of fast-decaying excitation from P. The model results will not change if there is

a reciprocal slowly decaying inhibition from I_2 to I_1, or a fast- or slow-decaying inhibition from I_1 to P. This model is also discussed in Bose et al. (2000).

Basic Assumptions

The models operate with very few restrictions. However, there are three necessary assumptions.

Assumption 1

Theta frequency can be modulated by running speed of the animal, but it is context-dependent. For behavior on linear tracks, King et al. (1998) showed that certain cells in the medial septum have a firing frequency that changes linearly with running speed. These data suggest that the theta rhythm itself could change linearly with running speed. We assume this to be the case only when the animal is running on a linear track. For behavior in the wheel, Czurkó et al. (1999) showed that theta frequency does not change with changes in running speed, which we assume.

Assumption 2

Interburst frequency of pyramidal cells increases linearly as a function of the theta rhythm. This implies that on the track, the interburst frequency of the pyramidal cells increases with running speed, since the theta frequency is assumed to change. Hirase et al. (1999) showed that interburst frequency of pyramidal cells does not change with running speed for a rat running in a wheel. This is consistent with our assumption, since the theta frequency is constant in this case.

Assumption 3

There must exist at least one slowly decaying current with particular properties in each of the networks. In network I, this current is, for example, a high-threshold inward calcium current intrinsic to P. In networks II and III, the current is synaptic and must target the pyramidal cell. In the Discussion, we will provide more details about the necessary properties of the slow current.

RESULTS

Overview of Model Results

Each of the models that we consider is capable of producing three distinct firing patterns. Two of these patterns are stable behaviors of the networks: out-of-place field behavior and in-wheel behavior; the third pattern is a transient pattern of firing corresponding to behavior inside the place field of an animal moving on a linear track. Each pattern is characterized by a unique functional relationship in which one of the elements T (for out-of-place field), D (for in-wheel), or P (for in-place field) controls the activity of the interneurons. The different controls allow inhibition within the network to be expressed in different ways. The transition between the different behavioral states corresponds to a change in control within the model network. There are two important changes in control in our networks. One occurs in the transition from out-of-place field to in-place field behavior, which is externally triggered at the beginning of the place field of P and allows P to take control of the firing pattern of the interneurons from T. The second occurs in the transition from in-place field to out-of-place field behavior. This is an emergent property of the network. The change occurs after 360° of precession and returns the control of the interneurons to T from P. In each of the models, the synapses between neurons are fixed and do not exhibit plasticity. The changes in control result from changes in the timing of the interactions between neurons, and not from changes in the strength of these interactions.

The dynamics of each model are straightforward. During out-of-place field behavior, P does not fire, while interneurons fire by postinhibitory rebound. Some or all of the interneurons in this state are driven by T, which thus controls network activity. Transient in-place field behavior is initiated by a one-time dose of excitation from D to P. Once in the place field, the phase of P's firing precesses relative to the underlying theta rhythm. The precession occurs because the frequency of pyramidal cell firing is higher than that of the theta rhythm. These frequencies are assumed to be modulated by running speed. Some interneurons fire due to the excitation from the phase-precessing P and thus also phase-precess. As a result, during the early cycles of phase precession, these interneurons are moved to a phase at which they are insensitive to T input. Each model possesses a mechanism which detects when the pyramidal cell and the interneurons have phase-precessed through nearly 360°. When this occurs, the interneurons are again at a phase where they can fire by postinhibitory rebound. At this cycle, the control of the network can be recaptured by T, returning the network to a stable steady state. The time, and thus spatial location, at which this change of control occurs are determined by the models without any further external input. Thus the determination of the spatial location of the end of the place field is an emergent network property. The in-wheel behavior is characterized by D controlling the network by forcing the pyramidal cell and interneuron to phase-lock well before 360° of precession. In this situation, the rat is assumed to be running in a wheel which is completely stationary with respect to the background environment. Furthermore, we assume that the rat is fixed at the beginning of a place field (see Discussion). Therefore, the dentate will provide a periodic signal to P, forcing it to phase-lock to the underlying theta rhythm.

In order to convey the main ideas of this paper, we shall describe in detail only the dynamics of network I. We will then give brief descriptions on how similar ideas apply to networks II and III. We assume for now that the running speed of the animal is constant. Later, we show how to account for changes in the animal's running speed.

Out-of-place field behavior

When the animal is running on a linear track but is outside of the associated place field, the place cell exhibits a low firing rate. In the model, this physical situation corresponds to a dynamic pattern in which the pacemaker T drives I at the theta frequency, but P

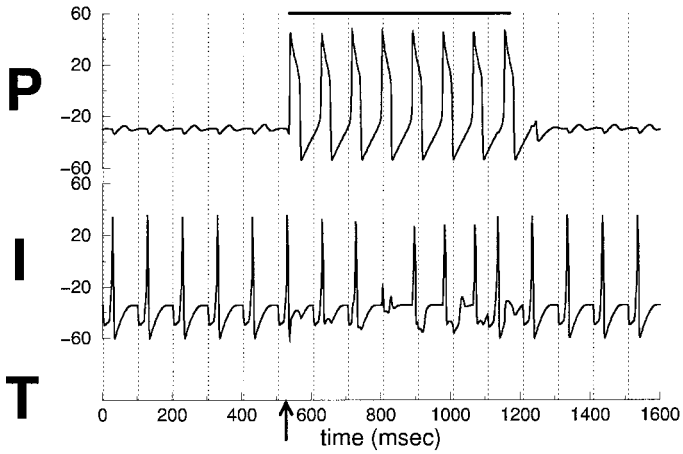


FIGURE 2. Firing pattern of cells when the rat is running on a linear track. Place field occurs beneath the solid line above the *P* voltage trace. The *T* spikes are not shown but are indicated by dotted vertical lines. At $t = 525$ ms, a one-time dose of excitation from *D* to *P* (arrow), signalling the beginning of the place field, causes *P* to fire. Notice that *P* and *I* phase precess over the next 8 cycles. The lower spike heights for *I* around 600–1,100 ms show that the inhibition from *T* to *I* is still present, but is hitting *I* in its active state. At 800 ms, the inhibition from *T* cancels the excitation from *P*, and *I* remains silent. The end of the place field is signalled by the recapture of *I* by *T* after nearly 360° of precession, near $t = 1{,}200$ ms.

never fires. This pattern is the default behavior of the model network and is displayed during the first 525 ms and last 400 ms of Figure 2. As seen in Figure 2, *I* spikes via postinhibitory rebound after being released from the fast inhibition from *T*. Once active, *I* provides fast-decaying inhibition to *P*. We assume that *P* does not fire by postinhibitory rebound. In this case, the pacemaker *T* controls the activity of *I* and, thus, network behavior. This firing pattern represents a stable dynamic state of our minimal network, and we call it the *TIP* orbit. Notice that outside of the place field, the synaptic connection from *P* to *I*, while present, is never activated.

Phase precession, transients, and place cells along a linear track

Within the place field, the firing phase of *P* systematically precesses through up to 360° and then *P* stops firing. We first discuss why the pyramidal cell is capable of firing when the animal is in the place field. This occurs if *P*, instead of *T*, controls the activity of *I*. This switch in control is initiated by a one-time burst of excitation from the dentate gyrus (D), which projects to place cells and signals the entrance into the place field ($t = 525$ ms in Fig. 2). The input from the dentate gyrus is known to occur at a specific phase of the theta rhythm (Skaggs et al., 1996) and can be thought of as a seed for a memory recall (Marr, 1971; McNaughton and Morris, 1987). In our model, the seed fires 90° after the peak of *T* firing, and provides excitation to *P*, causing it to fire. Once *P* fires, it activates the high-threshold inward current which provides *P* with a long-lasting depolarizing current. We assume that this current persists for at least one theta cycle and is strong enough to keep *P* in the oscillatory regime. Thus *P* can fire again, which renews the effect of the high-threshold current and allows the process to repeat.

The effect of this seed input is to reorganize the functional roles of the cells within the network. Once *P* fires, it causes *I* to fire earlier than it did outside of the place field. As a result, the timing of the *T* to *I* and the *I* to *P* inhibition is changed. Whenever *P* fires *I*, the inhibition from *I* to *P* occurs when *P* is in its active state, and largely insensitive to the inhibitory input. So as long as *P* controls the activity of *I*, *P*'s behavior will be dictated by its intrinsic dynamics, which are now those of an oscillator. The in-place field dynamics are shown in Figure 2, and we call this the *PIT* orbit.

We now provide conditions under which place cells phase-precess. In particular, we focus on the transient nature of phase precession and place-cell firing. One of the main issues we address is the following. In the absence of a priori information about the length of the place field, what mechanism(s) determines the end of the place field? Below, we suggest that 360° of precession signals the end of the place field.

Denote the period of *P* by T_P and of *T* by T_T. We restrict to the situation $T_P < T_T$. This is a sufficient condition for phase precession. In Bose et al. (2000), it is shown that if $T_P > T_T$, then precession can occur if the time constant of decay of the inhibitory synapse from *I* to *P* is larger than the time constant of the calcium current responsible for the burst width of an action potential. Once *P* has taken control of the activity of *I*, both cells phase precess relative to *T*; *P* precesses because $T_P < T_T$, and *I* precesses since it fires whenever *P* does. Notice that within the place field, *P* fires before *I* does, which is consistent with the experimental findings of Csicsvari et al. (1998) (see Fig. 2 and Discussion). Also, see Bose et al. (2000) for precise conditions on the phase relationship between *D* and *T*, the amount of phase precession per cycle, the expected number of cycles of phase precession as a function of relevant parameters in the network, the total amount of phase precession, and other details of this network phenomenon. In particular, the phase advance at each cycle is given by $360° (T_T - T_P)/T_T$.

Place cells stop precessing when *T* recaptures *I*. The experimental results of O'Keefe and Recce (1993) show that place cells precess through up to 360°. Our model is designed to use this fact, but as it applies to interneurons. In particular, when the animal is outside the place field, *I* lies near its rest state and in a position to respond to inhibitory input from *T*. When the animal is inside the place field, however, *I* phase-precesses. Thus *I*'s first firing due to *P* moves it away from a state where it can respond to *T*. In other words, the inhibitory input from *T* to *I* is no longer correctly timed to initiate a rebound spike. Within the place field, the first cycle of inhibition from *T* to *I* occurs when *I* is in its active state and thus is largely insensitive to the inhibition. Over the next few theta cycles, due to the precession, the inhibition comes during *I*'s active state and then in the early parts of its refractory state. Eventually, *I* precesses through close to 360° and returns to a phase where it can respond to input from *T* (see Fig. 3). At this cycle, *I* fires a rebound spike.

The effect of *I* firing a rebound spike is to rechange the timing of the *I* to *P* inhibition. This inhibition now comes when *P* is in its refractory state and thus highly sensitive to inhibitory input. When

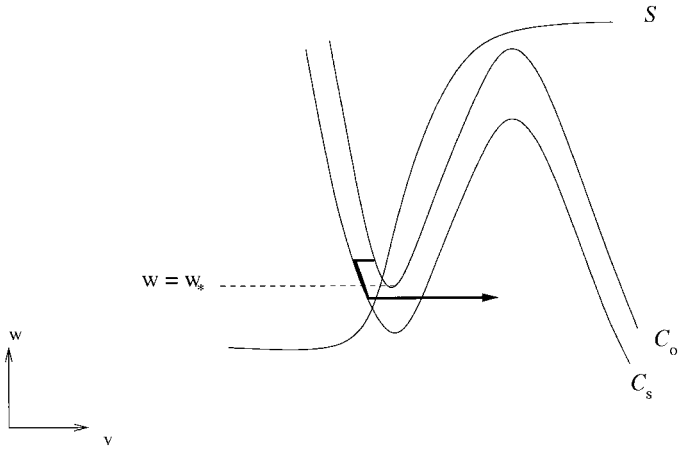


FIGURE 3. Relationship between length of fast inhibition and production of a postinhibitory spike. Dynamics of fast inhibition are illustrated in the *v–w* phase plane of *I* (see Appendix for equations). The upper cubic C_0 is the intrinsic *v*-nullcline of *I,* while the lower cubic C_s is the synaptically inhibited *v*-nullcline. The sigmoid-shaped curve S is the *w*-nullcline. Its intersection with either cubic forms a stable fixed point for *I*. The intersection of the sigmoid with C_0 can be assigned the value of 0° or 360°. When *I* receives inhibition, its voltage drops quickly (trajectory (thick line) moves horizontally to the left in the phase plane) and then travels slowly down the left branch of C_s. If at the point where the inhibition wears off, the trajectory (thick line) is such that $w < w_*$ then *I* fires a spike by postinhibitory rebound and ends up on the right branch of C_0. If not, *I* does not fire and returns to the left branch of C_0. Thus the time length of the inhibition to *I,* which determines how long it will move down the left branch of C_s, is a determinant of whether or not *I* can generate a rebound spike. The more substantial the inhibition, the greater the chance to rebound.

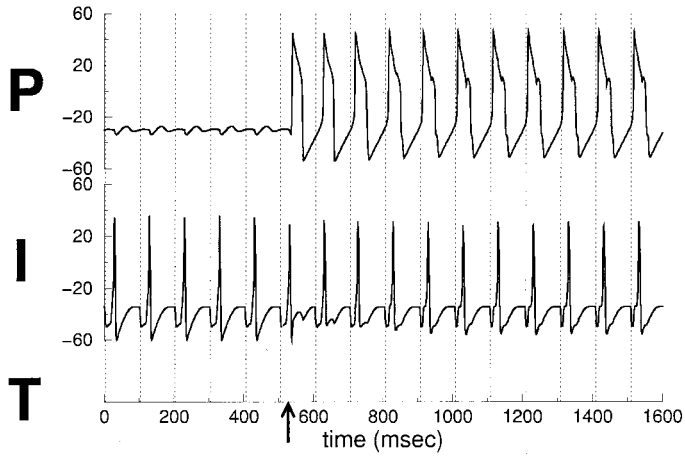


FIGURE 4. Firing pattern of cells when the rat is running in the wheel. At $t = 525$ ms (arrow), *P* receives an excitatory synaptic input from *D* (g_{dp} changed from 0 to 4), causing *P* to fire and precess for a few cycles. The wheel cell locks after approximately 60° of precession, when the excitation from *D* occurs at a time where it can extend the burst duration of *P*. Note the slight depolarization near the end of the *P* burst. Because the animal is spatially clamped, *D* continues to fire. The reduced spike heights of *I* show that the inhibition from *T* hits *I* in its active phase. Initial conditions and parameters, except for g_{dp}, are the same as in Figure 2.

delivered during *P*'s refractory state, the inhibition has the effect of delaying a potential *P* burst for as long as the inhibition is active. During this time, the high-threshold depolarizing current is given additional time to decay. In the model, this additional time is sufficient to take *P* outside of the oscillatory range. Thus the oscillations of *P* end, and the network returns to the stable *TIP* orbit.

It is seen how the precession of the interneuron provides the network with a mechanism to end phase precession. Moreover, since the end of phase precession also means the end of place-cell firing, the mechanism also provides means to determine the spatial extent of the place field. The initial change in control of *I* from *T* to *P*, which is externally imposed by the dentate gyrus, creates the opportunity for precession to occur. The second change in control, which is internally determined by the network, signals the end of the place field.

Wheel cells, phase locking, and entraining a faster oscillator by a slower one through excitation

To describe how our model captures wheel-cell behavior, we continue to use the same restriction as above, namely $T_P < T_T$, and we also assume that the rat is running at a constant speed within the wheel. We now show that our model predicts that wheel cells will fire tonically and phase-locked to the underlying theta rhythm.

To understand this, consider again the two reasons why *P* oscillates during precession: 1) it has the intrinsic ability to do so; and 2) the inhibition from *I* to *P* comes during *P*'s active phase. We showed above that the precession of *I* ultimately leads to a situation where *T* regains control of *I* and gives *P* inhibition at a phase which ends the pyramidal-cell oscillations. It follows that if the control of *I* never gets recaptured by *T*, then *P* will fire tonically. One way this can happen is if *P*'s firing becomes phase-locked to the underlying theta rhythm, thus prohibiting the change of *I* control to *T*.

In our model, the entrainment of *P* and *I* occurs when *D* modulates the firing of *P*. At the beginning of the place field and at a particular theta phase, say θ_0, the granule cell fires (Skaggs et al., 1996). When the phase of *T* returns to θ_0, the animal is still at the beginning of the place field, so the granule cell fires again, and so on. In Figure 4, we show the phase locking of wheel cells. Until $t = 525$ ms, the rat is assumed be outside the wheel cell's firing location and *P* does not fire. At $t = 525$ ms, *T* fires and we change the maximal conductance of the synaptic current from *D* to *P* from zero to four. The granule cell is also periodic with period T_T, but its initial conditions are chosen such that its firing peak is 25 ms (90°) after the peak of *T* firing. This allows *D* to periodically excite *P* at the theta frequency. Note that *P* precesses through roughly 60° before it phase-locks. We call this the *PID* orbit.

We mentioned earlier that the target of control is the interneurons. While *P* controls the firing pattern of the interneuron in the wheel, it can only retain control due to the periodic input from *D*. So it is most appropriate to say that *D* has control of the network in the wheel.

The entrainment of *P* by the dentate gyrus is somewhat counterintuitive. The period of firing of granule cells is T_T, while the intrinsic period of *P* is T_P, where $T_P > T_T$. Thus the *excitation*

from the granule cell *slows down* the oscillations of the faster *P* cell. The reason this occurs is that the excitation hits the wheel cell when *P* is near the end of its intrinsic burst, and thereby prolongs the burst duration. When the animal first enters the wheel, the excitation from *D* initiates firing. The next dose of excitation from *D* comes during the early part of the active phase of *P*, since $T_P < T_T$. Eventually, *P* precesses to a phase at which the dentate input is capable of extending the burst duration of *P*. This causes the period of *P*'s oscillation to become larger and causes the phase-locking. Hirase et al. (1999) did not discuss the early part of the data when the rat first enters its associated place field in the wheel, and thus report only that wheel cells phase-lock. Our analysis suggests that during the early part of the firing, wheel cells phase-precess through a number of degrees before becoming entrained to the theta rhythm.

One can obtain an upper bound on the amount of phase precession wheel cells should undergo. Let τ_P denote the time duration of the active state of the intrinsic *P* cell. The duty cycle of a cell is defined to be the fraction of time it spends in the active state vs. the total period. For *P*, the duty cycle is then τ_P/T_P. Using a geometric analysis (details not shown), we establish that the maximum amount of precession of wheel cells is $\tau_P/T_P\ 360°$. Determining the minimum amount of precession is less straightforward. It depends primarily on the burst duration of *D*, the maximal conductance of the *D* to *P* synapse, and the decay time constant of the excitatory current from *D* to *P*. The larger any of these parameters, the less precession the wheel cell undergoes. The reason is that increasing any of these parameters lengthens the burst duration of *P*. This means that the timing at which the lengthening begins is earlier in a theta cycle, which means locking at a later phase.

Correlating phase with position through running-speed modulation

We now show how to correlate phase of place field firing with spatial location of the animal on a linear track through a speed modulation (correction) mechanism. For the sake of argument, assume that within the place field, *P* oscillates with frequency f_P, while *T* oscillates with frequency f_T. Suppose that both of these frequencies vary linearly with changes in the animal's running speed. In particular, let $f_T = f_B + \gamma_1 v$, $f_P = f_B + \gamma_2 v$, where $\gamma_2 > \gamma_1$ are positive constants. The velocity v is set to $v_0 + \Delta v$, where v_0 is the minimum velocity needed for the theta rhythm to exist, and Δv is the positive deviation from this baseline velocity. Without loss of generality, the frequency f_B is a common baseline for $\Delta v = 0$. Let $\gamma = \gamma_2 - \gamma_1$, then $f_P = f_T + \gamma v$, where $\gamma > 0$. The phase shift at each cycle of *P* firing is $\Delta\phi = 360° (f_P - f_T)/f_P$. Therefore, the total phase shift at the *n*th *P* cycle is $\phi_n = 360°(f_P - f_T)/f_P$. Using the above relation for the frequencies, we find that $\phi_n = 360° n\gamma v/f_P$. Note that the position of the rat at the *n*th cycle is $x_n = nv/f_P$. Therefore, the total phase shift and the position of the rat at the *n*th *P* cycle are related by $\phi_n = 360°\gamma x_n$. Thus the phase is correlated to the animal's position through the difference in the slopes γ. See Figure 5.

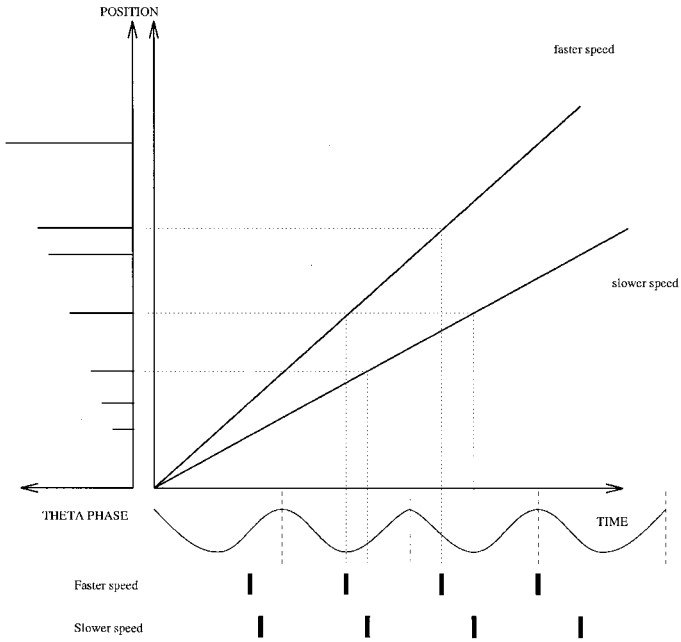


FIGURE 5. Correlating phase with location via changes in running speed. Two different running speeds are shown. Space and firing time of cells are correlated simply through the relationship distance = velocity*time. Note that the second spike of the faster-running animal corresponds to the same spatial location of the third spike of the slower-running animal. These locations occur at the same phase of the theta rhythm, but at different cycles. For the faster speed, the position is reached near the second local minima of the theta rhythm, while for the slower speed, the position is reached near the third local minima.

The above derivation assumes the animal can run through the place field at any given velocity, but that the velocity per trial during each passage is constant. The analysis can easily be extended to assume that the velocity varies during passage through a place field but remains constant on a cycle-by-cycle basis. Denote by v_n the velocity of the animal during the *n*th *P* cycle. Then the total phase shift is given by $\phi_n = 360° \sum_{k=1}^{n} [(f_P - f_T)/f_P]_k = 360° \sum_{k=1}^{n} \gamma v_k/f_{P_k}$. The position of the animal is now given by $x_n = \sum_{k=1}^{n} v_k/f_{P_k}$. Therefore, the total phase shift and position of the animal are still related by $\phi_n = 360°\gamma x_n$.

For the animal running in the wheel, there is no need for a speed correction mechanism, since neither the theta frequency nor the interburst frequency of wheel cells changes with running speed.

Other networks

We now briefly discuss two other network models that use the same ideas of control in order to achieve the dynamics described above. In each model, as above, *T* controls the *TIP* orbit, *P* controls the *PIT* orbit, and *D* controls the *PID* orbit. The mechanisms used to switch from *TIP* to *PIT* and *PID* are as above. There are differences in how each of the models operates, however, which are spelled out below.

Network II. For this network, *P* is an oscillator and I_2 fires if and only if I_1 fires by postinhibitory rebound. This can occur since I_1

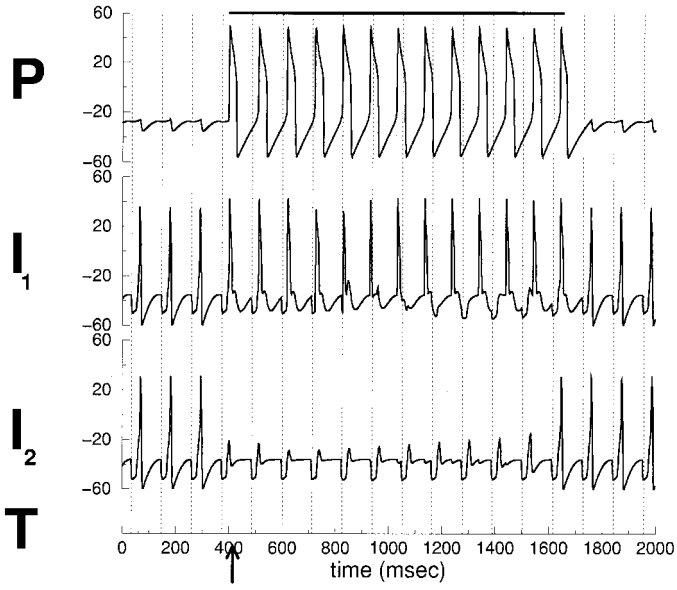


FIGURE 6. Simulation results, using network III for behavior on the linear track. The dentate provides a single excitatory input to *P* at $t = 400$ ms (arrow), and *P* and I_1 precess for the next 13 cycles (below solid line). The place field ends with the recapture of I_1 and I_2 by *T* near $t = 1{,}600$ ms.

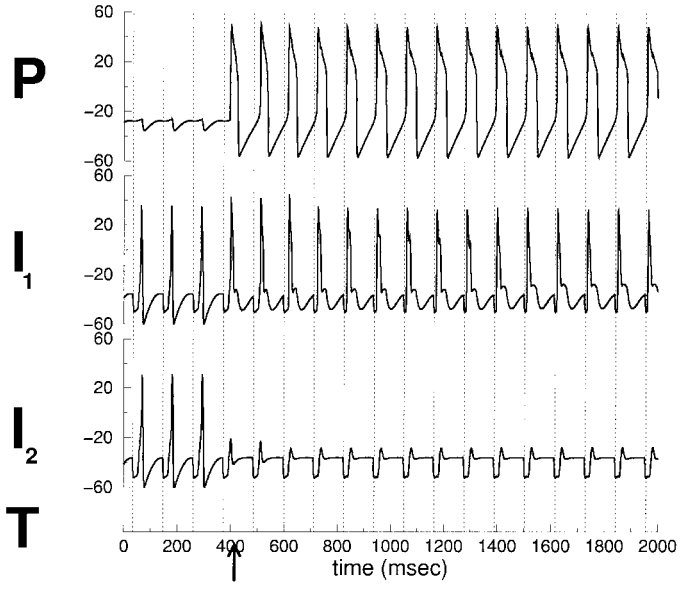


FIGURE 7. Simulation results, using network III for behavior in the wheel. Initial conditions are the same as in Figure 6. Now the dentate provides periodic input to *P*, beginning at $t = 400$ ms. The wheel cell precesses through about 60° before locking for the duration of the simulation.

fires either by postinhibitory rebound in response to *T*, or by excitation in response to *P*. In the former case, the width of I_1's action potential is longer, thus providing a longer duration of inhibition to I_2. As discussed in Figure 3, a longer duration of inhibition can cause a postsynaptic cell (I_2 in this case) to rebound spike.

In *TIP*, *T* fires I_1, which then fires I_2. The slowly decaying inhibition from I_2 to *P* prohibits *P* from firing and is renewed at each cycle. During *PIT*, *P* fires I_1, which does not fire I_2. Thus, the slow inhibition to *P* is functionally removed. As a result, *P* can oscillate at its intrinsic frequency for as long as it controls I_1. Similarly to network I, *T* regains control of I_1 after 360° of precession, which causes I_2 to fire and *P* to be suppressed. Changes in running speed are as before. The *PID* orbit results as before, because *P* phase-locks, and control of I_1 is never returned to *T*.

Network III. The main difference between network III and the previous two lies in how control of the interneurons is changed back from *P* to *T*. See Figures 6 and 7. Outside of the place field, both I_1 and I_2 fire spikes, with the slow inhibition from I_2 serving to suppress oscillations of *P*. The slow inhibition from I_1 to I_2 arrives during I_2's active phase and has enough time to decay away for I_2 to rebound-spike at the next theta cycle. Excitation from *D* causes *PIT* to begin. Now *P*'s first firing causes I_1 to fire earlier than it did in the *TIP* orbit. Thus the timing of the inhibition from I_1 to I_2 is changed so that at the next *T* spike, neither I_1 nor I_2 rebound-spikes. I_1 does not rebound because its phase relative to *T* has changed, and I_2 does not spike because it is being suppressed by the slowly decaying inhibition from I_1. Because I_1 phase-precesses, the inhibition that it provides to I_2 has progressively more time to decay away at each cycle of the theta rhythm. Eventually, *T* regains control of I_1 and I_2. This regain of control can happen in two ways. *T* can first regain control of I_1. This occurs for exactly the same reasons as in networks I and II, namely that the phase of I_1 has gone through 360° and is thus in a position to rebound (see Fig. 3). When it does, the timing of the I_1 to I_2 inhibition will return to the timing of the *TIP* orbit, and I_2 will fire, thus suppressing *P*. The second way the control can change is if *T* directly fires I_2 by rebound. This happens if enough of the I_1 to I_2 inhibition has decayed away, which occurs when I_2 fires sufficiently early in a theta cycle (see Fig. 8). The *PID* orbit occurs for the same reasons as above.

DISCUSSION

The above descriptions and simulations show that networks which use speed-modulated dynamics reproduce the firing patterns of hippocampal pyramidal cells. In order for these networks to operate in the various rhythmic states, a functional reorganization of the roles of the cells in the network must occur. We have shown that reorganization in roles occurs whenever a particular cell gains control of the network dynamics. A main finding of our work is the identification of biologically plausible explanations for what causes these changes in control. The neural mechanisms that we propose may not be the only ones which yield the needed functional relationships. In more detailed models, there may exist a number of strategies that a particular network uses to bring about the desired functional interactions.

The models we consider have minimal requirements and thus are representative of a large class of possible models. The primary

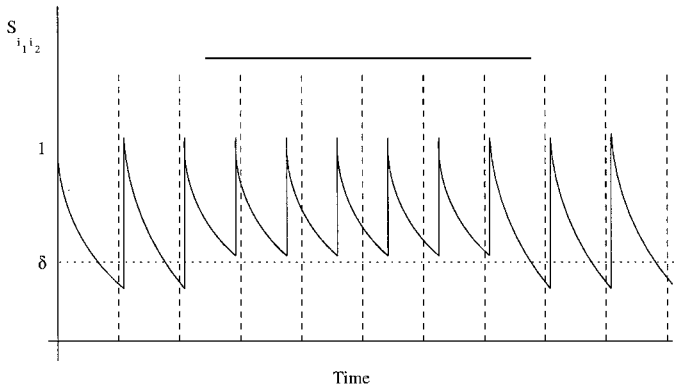


FIGURE 8. Dynamics of the synaptic current between I_1 and I_2, and its temporal relationship with T. T firing is shown by dashed vertical lines. T can only cause I_2 to fire by postinhibitory rebound if the synaptic current from I_1 to I_2, $s_{i_1 i_2}$, intersects the dotted line below a prescribed value δ. Overbar indicates place field. Within the place field, progressively more of the inhibition from I_1 to I_2 decays at each cycle of the precession. Each time P and I_1 fire, $s_{i_1 i_2}$ is renewed to a value 1, and then decays with a fixed time constant. During phase precession, this input arrives with a higher frequency. This provides a mechanism to return to the out-of-place field physiology after 360° of phase precession.

requirements are modulation in theta and pyramidal-cell frequencies due to changes in running speed, and the existence of at least one long time constant with particular properties. The long time constant targets the pyramidal cell, but plays different roles in each of the three networks. In network I, it provides long-lasting depolarization to the pyramidal cell within the place field. In network II, it provides long-lasting inhibition to the pyramidal cell outside of the place field. In network III, there are two long time constants. The first inhibits pyramidal cell activity outside of the place field as in network II. The second provides long-lasting inhibition within the place field to the interneuron responsible for suppressing place-cell activity. In all cases, the functional enhancement or removal of the slowly decaying current associated with the long time constant provides the pyramidal cell the opportunity to phase-precess. In more realistic networks of neurons, some or all of the long time constant properties described may actually be used.

Advantages of a Temporal Process

One of the main advantages of the temporal approach to pyramidal cell firing is that it shows how networks of neurons construct information. Namely, the network is able to take a limited amount of spatial information and return more precise information about the location of the animal over a larger spatial extent. With respect to precession, the network is given two pieces of external information, the beginning of the place field and the speed of the animal. With these inputs, the network is able to accurately determine the length and end of the place field, as well as the animal's position within this place field. The network is given no a priori information about the length of the place field. Instead, it is the internal dynamics of the network which determine that the place field has ended when the pacemaker recaptures control of the interneurons after 360° of precession. Identical pyramidal cells will have equal-length place fields if they interact with distinct but identical interneuron networks. Cellular and network heterogeneities, however, can contribute to produce place fields of different lengths.

With respect to phase-locking, the network is able to determine that the animal is "clamped" in space. Since phase and location are correlated with one another, the fact that wheel cells phase-lock signals to the animal that its location is fixed in space. The model also shows that the wheel cells only lock when the animal is at or near the beginning of the place field (see below).

Predictions

The first prediction of this model is that pyramidal cell firing can accurately be described as a temporal process in which the timing of bursts is modulated by the animal's running speed. There are several ways to test this prediction. For instance, if a rat is running on a linear track and turns around in the middle of a unidirectional place field, then we predict the pyramidal cell will continue firing even though the animal is no longer in the place field of that cell. As another example, if after place fields are recorded on a stationary linear track, the rat is made to run without spatial translation on a now moving track, then this model predicts that within a fraction of the initial spatial extent of the place field, the cell will now fire phase-locked to the theta rhythm. If the rat is made to run in place in the remainder of the place field, the prediction is that the cell will complete the phase precession and stop firing.

The second prediction is that a subset of interneurons may also phase-precess when the rat is in the place field of a place cell. The firing patterns of these interneurons in general may not be phase-correlated, but there may exist a small time window in which their firing contains phase information. Csicsvari et al. (1998) found place cell-interneuron pairs in which the firing of the place cell *precedes* the firing of the interneuron by tens of milliseconds. This finding is consistent with our prediction that interneurons may phase-precess in the place field, as this is precisely where the firing of interneurons is controlled by and preceded by the place cell. This prediction is *not* inconsistent with the finding of Skaggs et al. (1996), who found that *on average,* interneurons do not phase-precess.

The third prediction is that the wheel cell locks at a phase which predicts a future location of the animal. If the animal is stuck at the beginning of a place field, then the dentate granule cells provide periodic excitation to the wheel cell. As demonstrated, this causes the wheel cell to fire tonically, since control of the interneurons never returns to the pacemaker. The phase at which the wheel cell locks to the theta rhythm is not the initial phase of firing of the cell. Instead, the wheel cell phase-precesses through a number of cycles, up to τ_P / T_P 360°, before locking. Thus the wheel cell phase-locks at a phase that represents a future location of the animal. If we use the results of Skaggs et al. (1996) to the effect that granule cells fire phase-precessed for a few cycles of theta, then we do not require the animal to be stuck at the beginning of the place field. In this case, the locked phase will be closer to the correct phase. Hirase et al. (1999) did not consider the first 1 or 2 s of their data, when the rat first enters the wheel. Thus they did not report seeing any preces-

sion in the wheel. Our results suggest that there is some amount of precession. There is a range of early phases at which the wheel cell can lock. As discussed earlier, determination of these phases depends on intrinsic characteristics of *D* and on properties of the *D* to *P* synapse. Our results do predict that there are later phases of precession during which the wheel cell cannot lock. We note, however, that this latter prediction may not be hold in a more detailed neuronal model.

The fourth prediction is that abrupt changes in distal visual cues outside of the wheel will cause the wheel cell to phase-precess through the full 360° before it stops firing. A sudden change in distal cues causes the input from *D* to *P* to seize, since sensory input from the entorhinal cortex to the dentate gyrus would change. This, in turn, causes the burst duration of *P* to return to its intrinsic duration, and allows the precession to begin again. Interestingly, Czurkó et al. (1999) demonstrated that the wheel cell stops firing when certain visual cues are changed. The changes they made were between trials, as opposed to during a single trial. In cases where the cues are removed during a trial, at issue is whether there is a time lag between the removal of cues and stoppage of firing with an accompanying phase precession, or whether the wheel cell immediately stops firing. The former would point to a temporal process, the latter, to a spatial process. Hirase et al. (1999) also found that certain changes in visual cues made a few wheel cells change their phase of firing as opposed to stopping their firing. The current versions of our models cannot account for this observation.

Relation to Prior Spatial Models

A variety of different models have been proposed to explain the phase-precession phenomena (Tsodyks et al., 1996; Jensen and Lisman, 1996; Wallenstein and Hasselmo, 1997; Kamondi et al., 1998). It is generally difficult to draw comparisons between models, as individually they set out to replicate or understand different aspects of function or physiology. All of the prior models were successful at producing phase precession in place cells, but the present model differs in the way that this precession is initiated and maintained. Unlike prior models, the correlation between the phase of place-cell firing and the animal's location in the present model is generated from a single spatially tuned input. A spatially coded phase is computed from the combination of this single spatial trigger, and speed information that arrives at place cells from a different anatomical pathway. In this way the spatial code is generated in the place cells. In prior models the spatial information was transmitted to the place cells continuously from a single pathway, which contained as much information upstream, as was present in the phase precession. All of the prior models, and the present model, predict phase-locking of wheel cells.

In Tsodyks et al. (1996) and Jensen and Lisman (1996), a one-dimensional, unidirectional chain of coupled place cells is considered. Each place cell encodes a location along the track, with the ordering of place cells corresponding naturally to the ordering of locations along the track. At each theta cycle, excitation is provided to a subsequent and specific member of the chain, which in turn excites the next member of the chain. Thus the phase precession is externally supplied by the fact that the external excitation moves down the chain of oscillators, thus causing members of the chain to fire at earlier theta phases than they did at the previous cycle. While these models would predict that wheel cells fire phase-locked to theta, they also predict that all cells further down the chain, which code for all future locations in space, would also fire. They do not predict phase advancement of wheel cells, unless the dentate granule input itself precesses.

The model of Wallenstein and Hasselmo (1997) also predicts phase-locking in wheel cells, but only if the external input to the network is phase-locked. The model of Kamondi et al. (1998) also predicts that wheel cells should phase-lock. However, if the animal is stuck at the beginning of the place field, then the model predicts that wheel cells should exhibit no phase advancement, i.e., wheel cells should lock at the initial phase. However, if the animal is actually partially in the place field, then the model predicts that wheel cells lock at a earlier phase and thus do exhibit some amount of precession.

In our prior work (Bose et al., 2000), the effects of synaptic delays were considered, but for simplicity we have ignored them here. For these minimal models of the phase precession of a single place cell, delays are not important. The main effect of the delay would be to globally shift the phase relationship of *P*, *I*, I_1, and I_2 relative to *T*. For example, with delays incorporated, *P* may begin firing at 100° relative to theta instead of 80°. Delays would not change the qualitative firing properties shown above, or the functional relationships needed to achieve them. Delays will need to be considered and will become functionally relevant when considering larger networks of cells and pattern-completion processes. Their exact role will be elucidated in future work.

The other effect that we have not included is the experimental result that the firing rate of place cells increases as the rat nears the middle of the place field and then decreases as it leaves the middle (O'Keefe and Burgess, 1996). That is, place cells fire more spikes within a burst when the animal is near the center of the place field. However, the firing rate alone is not sufficient to pinpoint the location of the animal. There is some amount of controversy as to whether the phase of firing alone is sufficient. Future experimental and theoretical work needs to be done to determine whether or not the firing rate plus phase of firing conveys more information about the rat's location than just the phase of firing alone.

Acknowledgments

We thank Victoria Booth for numerous helpful insights and suggestions.

REFERENCES

Alonso A, Kohler C. 1982. A study of the reciprocal connections between the septum and the entorhinal area using anterograde and retrograde axonal transport methods in the rat brain. J Comp Neurol 225:327–343.

Bose A, Booth V, Recce M. 2000. A temporal mechanism for generating the phase precession of hippocampal place cells. J Comput Neurosci 9:5–30.

Brown E, Frank L, Tang D, Quirk M, Wilson M. 1998. A statistical paradigm for neural spike train decoding applied to position prediction from ensemble firing patterns of rat hippocampal place cells. J Neurosci 18:7411–7425.
Claiborne B, Amaral D, Cowan W. 1986. A light and electron microscope analysis of the mossy fibers of the rat dentate gyrus. J Comp Neurol 246:435–458.
Csicsvari J, Hirase H, Czurkó A, Buzsaki G. 1998. Reliability and state-dependence of pyramidal cell-interneuron synapses in the hippocampus: an ensemble approach in the behaving rat. Neuron 21:179–189.
Czurkó A, Hirase H, Csicsvari J, Buzsaki G. 1999. Sustained activation of hippocampal pyramidal cells by "space clamping" in a running wheel. Eur J Neurosci 11:344–352.
Freund TF, Buzsáki G. 1996. Interneurons of the hippocampus. Hippocampus 6:347–470.
Hirase H, Czurkó A, Csicsvari J, Buzsáki G. 1999. Firing rate and theta-phase coding by hippocampal pyramidal neurons during "space clamping." Eur J Neurosci 11:4373–4380.
Jensen O, Lisman JE. 1996. Hippocampal CA3 region predicts memory sequences: accounting for the phase advance of place cells. Learn Mem 3:257–263.
Jung MW, McNaughton BL. 1993. Spatial selectivity of unit activity in the hippocampal granular layer. Hippocampus 3:165–182.
Kamondi A, Acsady L, Wang X, Buzsáki G. 1998. Theta oscillations in somata and dendrites of hippocampal pyramidal cells in vivo: activity-dependent phase-precession of action potentials. Hippocampus 8:244–261.
King C, Recce M, O'Keefe J. 1998. The rhythmicity of cells of the medial septum/diagonal band of broca in the awake freely moving rat: relationship with behaviour and hippocampal theta. Eur J Neurosci 10: 464–467.
Marr D. 1971. Simple memory: a theory for archicortex. Philos Trans R Soc Lond Biol 176:23–81.
McNaughton BL, Morris RGM. 1987. Hippocampal synaptic enhancement and information storage within a distributed memory system. Trends Neurosci 10:408–415.
Mehta M, Quirk MC, Wilson MA. 2000. Experience-dependent asymmetric shape of hippocampal receptive fields. Neuron 25:707–715.
Morris C, Lecar H. 1981. Voltage oscillations in the barnacle giant muscle fiber. Biophys J 35:193–213.
O'Keefe J, Burgess N. 1996. Geometric determinants of the place fields of hippocampal neurons. Nature 381:425–428.
O'Keefe J, Dostrovsky J. 1971. The hippocampus as a spatial map. Preliminary evidence from unit activity in the freely-moving rat. Brain Res 34:171–175.
O'Keefe J, Recce ML. 1993. Phase relationship between hippocampal place units and the EEG theta rhythm. Hippocampus 3:317–330.
Shute C, Lewis P. 1963. Cholinesterase-containing systems of the brain of the rat. Nature 199:1160–1164.
Skaggs WE, McNaughton BL, Wilson MA, Barnes CA. 1996. Theta-phase precession in hippocampal neuronal populations and the compression of temporal sequences. Hippocampus 6:149–172.
Swanson LW, Cowan WM. 1976. Autoradiographic studies of the development and connections of the septal area in the rat. In: DeFrance J, editor. The septal nuclei: advances in behavioral biology. Plenum Press.
Traub R, Miles R. 1991. Neuronal networks of the hippocampus. Cambridge: Cambridge University Press.
Tsodyks MV, Skaggs WE, Sejnowski TJ, McNaughton BL. 1996. Population dynamics and theta rhythm phase precession of hippocampal place cell firing: a spiking neuron model. Hippocampus 6:271–280.
Wallenstein GV, Hasselmo ME. 1997. Gabaergic modulation of hippocampal population activity: sequence learning, place field development, and the phase precession effect. J Neurophysiol 78:393–408.
Wang XJ, Rinzel J. 1992. Alternating and synchronous rhythms in reciprocally inhibitory neuron models. Neural Comp 4:84–97.
Wong R, Prince D. 1978. Participation of calcium spikes during intrinsic burst firing in hippocampal neurons. Brain Res 159:385–390.
Zhang K, Ginzburg I, McNaughton B, Sejnowski T. 1998. Interpreting neuronal population activity by reconstruction: unified framework with applications to hippocampal place cells. J Neurophysiol 79:1017–1044.

APPENDIX

The equations that we used for the simulations are based on the equations of Morris and Lecar (1981). For Figures 2 and 4 involving the simulations of network I, the pyramidal cell is described by a set of four first-order equations which contain channels for a leak, potassium, calcium, and a high-threshold inward current. The equations are:

$$C_m \frac{dv_p}{dt} = -g_{Ca} m_{\infty,p}(v_p)[v_p - v_{Ca}] - g_K w_p[v_p - v_K] - g_L[v_p - v_L] - g_h h[v_p - v_h] + I_{\text{ext}} + I_{\text{syn}}, \quad (1)$$

$$\frac{dw_p}{dt} = \epsilon[w_{\infty,p}(v_p) - w_p]/\tau_{w,p}(v_p), \quad (2)$$

$$\frac{dh}{dt} = \alpha_h[1 - h]H_\infty(r - r_h) - \beta_h h H_\infty(r_h - r), \quad (3)$$

$$\frac{dr}{dt} = \alpha_r[1 - r]H_\infty(v_p - v_\theta) - \beta_r r H_\infty(v_\theta - v_p) \quad (4)$$

where v_p denotes voltage, w_p denotes the fraction of open potassium channels, h denotes the fraction of open high-threshold channels, and r determines the length of time for which these channels are open. The interneuron, pacemaker, and dentate granule cell are each described using only two first-order equations, as given by

$$C_m \frac{dv_x}{dt} = -g_{Ca} m_{\infty,x}(v_x)(v_x - v_{Ca}) - g_K w_x[v_x - v_K] - g_L[v_x - v_L] + I_{\text{ext}} + I_{\text{syn}}, \quad (5)$$

$$\frac{dw_x}{dt} = \epsilon[w_{\infty,x}(v_x) - w_x]/\tau_{w,x}(v_x), \quad (6)$$

where $x = i$, t, and d. Here $m_\infty(v) = \frac{1}{2}\left[1 + \tanh\left(\frac{v - v_1}{v_2}\right)\right]$, $w_{\infty,x}(v) = \frac{1}{2}\left[1 + \tanh\left(\frac{v - v_{3,x}}{v_{4,x}}\right)\right]$, and $\tau_{w,x}(v) = \frac{1}{\text{sech}[(v - v_{3,x})/2v_{4,x}]}$, and $H_\infty(v) = 0$ if $v \leq 0$ and $H_\infty(v) = 1$ if $v > 0$. Common parameter values are $C_m = 4.5$, $V_{Ca} = 120$, $V_K = -84$, $V_L = -60$, $g_{Ca} = 4.4$, $g_K = 8$, $g_L - 2$, $v_1 = -1.2$, $v_2 = 18$, and $\epsilon = 0.0225$. For t and d, $I_{\text{ext}} = 92$, for i, $I_{\text{ext}} = 85$, and for p, $I_{\text{ext}} = 80$, where I_{ext} represents an external applied current. For $x = p$, t, and d, $v_{3,x} = 2$ and $v_{4,x} = 30$. For $x = i$, $v_{3,x} = -25$ and $v_{4,x} = 10$. With these parameters, $T_T = 100.5$ ms. Other parameters are $g_h = 0.2$, $v_h = 100$, $\alpha_h = 5$, $\beta_h = 5$, $\alpha_r = 5$, $\beta_r = 0.011$, $x_h = 0.5$, and $v_\theta = -10$.

Each synaptic current I_{syn} has the form $-g_{xy}s_{xy}(v_x - v_{\text{syn}})$, where the variable s_{xy} obeys

$$s'_{xy} = \alpha_{xy}[1 - s_{xy}]\frac{1}{2}\left[1 + \tanh\left(\frac{v_x - v_{5,x}}{v_{6,x}}\right)\right] - \beta_{xy}s_{xy}, \quad (7)$$

where x denotes the presynaptic cell and y the postsynaptic cell. The parameters g_{xy} and v_{syn} are the conductances and reversal potentials of these currents. The common reversal potentials for the fast-decaying inhibitory synapses are $V_{\text{syn}} = -80$. For the excitatory synapse from P to I, we used $V_{\text{syn}} = 0$, and from D to P, $V_{\text{syn}} = 20$. The values for conductances and rise and decay rates α_{xy} and β_{xy} are $g_{pi} = 2$, $\alpha_{pi} = 2$, $\beta_{pi} = 1$, $g_{ip} = 0.1$, $\alpha_{ip} = 1.15$, $\beta_{ip} = 0.1$, $g_{ti} = 2.5$, $\alpha_{ti_1} = 2$, $\beta_{ti_1} = 2$, and $g_{dp} = 4$ at the beginning of the place field and 0 everywhere else, $\alpha_{dp} = 2$, and $\beta_{dp} = 2$. The other parameters are $v_{5,p} = 20$, $v_{6,p} = 10$, $v_{5,i} = 0$, and $v_{6,i} = 2$, and for both t and d, $v_{5,x} = 20$ and $v_{6,x} = 2$.

For Figures 6 and 7 involving simulations of network III, we used Equations (5) and (6) for all cells. The parameter values are the same as above, except for the following changes: $C_m = 5$, $\epsilon = 0.02$, for i_1 and i_2, $I_{\text{ext}} = 83$, $v_{4,x} = 11$, and for p, $I_{\text{ext}} = 100$. Here $T_P = 113$ ms and $T_T = 103$ ms. The synapses are governed by Equation (7) with the following values: $g_{i_1i_2} = 0.225$, $\alpha_{i_1i_2} = 4$, $\beta_{i_1i_2} = 0.0072$, $g_{pi_1} = 2$, $\alpha_{pi_1} = 1$, $\beta_{pi_1} = 0.1$, $g_{i_2p} = 0.4$, $\alpha_{i_2p} = 2$, $\beta_{i_2p} = 0.005$, $g_{ti_1} = 2.5$, $\alpha_{ti_1} = 2$, $\beta_{ti_1} = 2$, $g_{ti_2} = 3$, $\alpha_{ti_2} = 2$, $\beta_{ti_2} = 2$, and $g_{dp} = 1$ at the beginning of the place field and 0 everywhere else, $\alpha_{dp} = 2$, and $\beta_{dp} = 1$. The other parameters are $v_{5,p} = 20$, $v_{6,p} = 10$. For $x = i_1, i_2$, $v_{5,x} = 0$, and $v_{6,x} = 2$, for both t and d, $v_{5,x} = 20$ and $v_{6,x} = 2$. The reversal potential for the excitatory synapses is set at $V_{\text{syn}} = 80$, and for the slow inhibitory synapse at $V_{\text{syn}} = -95$.